



Simulating Ultra-High Energy Nuclei Propagation with CRPropa

SIGL, GUENTER¹, KAMPERT, KARL-HEINZ², KULBARTZ, JOERG¹, MACCIONE, LUCA³, NIERSTENHOEFER, NILS²

¹ *II. Institut für Theoretische Physik, Universität Hamburg, Luruper Chaussee 149, 22761 Hamburg, Germany*

² *University of Wuppertal, Gaußstraße 20, 42119 Wuppertal, Germany*

³ *DESY, Theory Group, Notkestraße 85, 22607 Hamburg, Germany*

guenter.sigl@desy.de

Abstract: Experimental data on the properties of Ultra-High Energy Cosmic Rays (UHECRs) above 10^{18} eV are open to controversial interpretations. Data on the elongation rate and its fluctuations, taken by the Pierre Auger Observatory, seem to indicate the possible presence of heavy nuclei in the UHECR spectrum. On the other hand, data on UHECR arrival directions seem to favor a lighter composition. It is therefore important to have tools to compute the propagation of UHECR nuclei in the InterGalactic Medium (IGM), that may help clarify these issues. To this aim, we extended the public code CRPropa to propagate heavy nuclei, taking into account all the relevant interactions they may undergo in the IGM and also their deflections due to intergalactic magnetic fields. We will show the first results of the new code, both on primary UHECR spectra and deflections and on the spectra of the secondary gamma-rays and cosmogenic neutrinos.

Keywords: CRPropa, UHE CR nuclei, ultra high energy cosmic ray propagation, secondaries simulation neutrino photon gamma, magnetic deflections

1 Introduction

Since the discovery of UHECRs the question about their origin and composition remains unanswered. Recently, the problem of composition was addressed by the Pierre Auger Observatory and by the High Resolution Fly's Eye (HiRes) exploiting the depth of the maximum X_{\max} of extensive air showers induced by UHECRs in the atmosphere. The Pierre Auger Observatory reports a gradual increase of X_{\max} as well as a decline of the width $\text{RMS}(X_{\max})$ above 3 EeV, indicating an increase of the average mass number A of UHECRs [1]. HiRes data on X_{\max} is instead compatible with a pure proton component [2]. Furthermore, the Pierre Auger Observatory reported an anisotropy (at 99% confidence level) on an angular scale $\psi \sim 3^\circ$ in the southern sky [3], but no such correlation has been found in the northern hemisphere (HiRes) [4]. At the highest energies where the X_{\max} measurements run out of statistics, anisotropies depend on composition, since the expected magnetic deflection grows with the charge of CR nuclei. Thus, a detailed understanding of the propagation of UHE-nuclei in a highly structured and magnetized IGM might help understand the reported anisotropy as well as the differing results of the relevant experiments.

Among others, these considerations motivated the extension of the publicly available version 1.4 of CRPropa, which was restricted to the case of primary UHE-protons, to allow for the propagation of UHE-nuclei up to iron. CRPropa v1.4 is a very good basis for this effort as many of its

features can be generalized to the case of UHE-nuclei: it is already able to compute the effects of photo pion and pair production in the extragalactic background light by UHE-nucleons and deflections in Extra Galactic Magnetic Fields (EGMF). Additionally, it is possible to simulate the propagation of secondary ν and γ -rays generated by interactions. These and other features of the code only needed to be slightly modified to allow for nuclei propagation. Moreover, it is required to introduce reactions which are specific to nuclei: photodisintegration, i.e. the splitting off of protons, neutrons and light nuclei from the mother nucleus in an inelastic scattering with a low energy background photon. Also, radioactive decays of the daughter nuclei had to be implemented. towards the observer within CRPropa.

2 Overview of CRPropa 2.0

As in the case of UHE-nucleons, UHE-nuclei lose energy in photo-pion and pair production reactions and are redshifted due to the expansion of the Universe. Additionally, nuclei photodisintegrate. In this reaction and in pion production unstable nuclei might be created and will decay subsequently. In order to handle correctly the case of nuclei propagation a realistic modeling of nuclear decay is therefore required. In this section, we only shortly describe the actual changes made to version 1.4 of CRPropa. For those features which remained unchanged, we refer the reader to the available publications on CRPropa version 1.4 [5].

Pair production (PP) is described as a continuous energy loss and is computed for protons from the secondary spectra given in [6]. For nuclei with charge Z , mass number A and energy E , the energy loss rate scales as [7]

$$\frac{\partial E_{A,Z}(\gamma)}{\partial t} = Z^2 \left(\frac{\partial E_p(\gamma)}{\partial t} \right). \quad (1)$$

Secondary electromagnetic cascades induced by pair production can also be simulated.

Also, *pion production* (π P) can be straightforwardly extended from nucleon to nuclear case. Since the center-of-mass energies involved in π P are much larger than the binding energy per nucleon, $E_B/A \approx 8$ MeV, we can neglect the binding energy and approximate π P as a reaction involving Z protons p and $(A - Z)$ neutrons n . The inverse mean free path λ^{-1} for pion production on a nucleus can then be written as an appropriate sum of the inverse mean free paths of the constituent nucleons

$$\lambda_{(A,Z)}^{-1} = Z\lambda_p^{-1} + (A - Z)\lambda_n^{-1}. \quad (2)$$

Here, the mean free path $\lambda_i = \lambda_i(\gamma)$ is again a function of the Lorentz factor and the subscripts (A, Z) , p, n denote the mean free path for a nucleus of mass number A and charge Z , or of a proton or neutron, respectively. If a pion production occurs, we use the event generator SOPHIA [8] to calculate the energy lost by the interacting nucleon (which subsequently leaves the primary nucleus) and to compute the non baryonic secondaries.

The most important interaction for nuclei is *photodisintegration* (PD). In a photodisintegration reaction nuclear fragments, mostly neutrons and protons, become dissociated from the parent nucleus. The dominant reaction channel is usually the resonant splitting off of a single nucleon, but in specific cases - especially at higher CR energies - other channels may become relevant. The needed photonuclear cross sections for $A \geq 12$ have been calculated using the numerical package TALYS [9]. For light ($A < 12$), stable nuclei we use parametrizations motivated in [10] or the total photo nuclear reaction channel as discussed in [11]. In the latter case, we assume the ejection of one proton if $Z > (A - Z)$ or of a neutron otherwise. In case of $A = 2Z$, both single nucleon channels are used with equal probability.

As stated above, photonuclear reactions may result in the production of unstable nuclei, which may then undergo *nuclear decay* (ND). In CRPropa 2.0, we use half life times and decay channels from the NuDat2 database [12] and we treat α and β^\pm decays, as well as p and n dripping. Additionally, nucleon dripping is used to move a nucleus towards the valley of stability if no information on that nucleus is available in the nuclear database.

In general, the length scales associated to the different interactions can differ by many orders of magnitude as a function of the energy and of the nucleus under consideration. This particularly applies to the case of the nuclear decay linked with widely varying half life times. In order to

guarantee an accurate and reasonably fast simulation procedure, we have implemented an *adaptive-stepsize propagation algorithm* which adjusts automatically according to the length scales at hand. The algorithm works as follows: using a random number $0 < p < 1$, we sample a timestep Δt_{int} after which an interaction takes place according to

$$\Delta t_{\text{Int}} = -\lambda \ln(p). \quad (3)$$

Here, the total mean free path $\lambda = (\sum \lambda_i^{-1})^{-1}$ is the inverse sum of the individual reaction rates λ_i^{-1} , where $i = \{\text{PD}, \pi\text{P}, \text{ND}\}$. However, Δt_{Int} in general is not equal to the propagation timestep Δt_{prop} , rather $\Delta t_{\text{prop}} \leq \Delta t_{\text{Int}}$. This limit is essentially due to two reasons: firstly, we must ensure that the propagated distance is less than the distance to the next observer. Secondly, we should ensure that the energy remains approximately constant during the timestep. In fact, because pair production is modeled as a continuous energy loss, a particle should lose energy during the propagation step. Neglecting this energy loss during the calculation of deflections results in a numerical error for the determination of the timestep Δt_{Int} as well as an error in the position finally reached after the propagation step. To ensure that these errors are small, it is necessary to impose the constraint $\Delta t_{\text{prop}} \leq \Delta t_{\text{Int}}$ on the maximum distance a particle may travel through EMGF before pair production losses are calculated.

3 CRPropa 2.0 showcase

CRPropa has many options to tune simulations to the specific needs of the user. The most important ones are the choice of either a one dimensional (1D) or a three dimensional (3D) environment, the choice of an observer (a sphere at a fixed distance from the source or an observer at a fixed position) and the choice of point like or continuously distributed sources. Among these options, the selection of a 1D or three 3D environment has the largest impact. Indeed, in a 1D simulation the distance and therefore the remaining propagation time to the observer is known in advance and therefore redshift dependent effects (e.g. cosmological evolution) can be taken into account. In 3D simulations one can calculate the deflections in Large Scale Structured (LSS) EGMF. In the following section we present example simulations to demonstrate some of these possibilities.

3.1 1D: Secondaries and Cosmological Evolution

In a 1D simulation it is possible to include source evolution and other redshift dependent effects. Additionally, the propagation of secondary electromagnetic cascades is numerically efficient since all cascades follow the same path and therefore the transport equation needs to be solved only once, at the end of the simulation.

As an example we present in figure 1 a simulation using two different cosmological evolution scenarios for the UHECR sources: a uniform scenario with constant

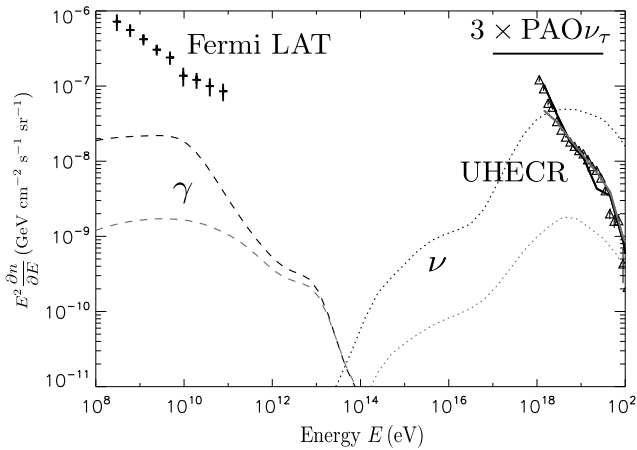


Figure 1: Spectra of primary cosmic rays (solid lines) and secondary ν (dotted lines) and γ (dashed lines) for two different continuous source evolution scenarios: FRII (black, upper lines) [13, 14] and an uniform source evolution (grey, lower lines). The triangles denote the UHECR spectrum measured by the Pierre Auger Observatory. For comparison, the Fermi LAT measurement of the extra galactic diffuse γ emission [15] and the upper limit on the UHE tau-neutrino flux from the Pierre Auger Observatory [16] multiplied by three are shown. For further details see text.

UHECR injection rate and a strong cosmological evolution scenario based on the evolution of Fanaroff-Riley II (FRII) radio galaxies [13, 14]. The primary cosmic ray component is injected with a mixed composition with galactic abundances and with a power law spectrum $dN/dE \propto E^{-\alpha}$ with $\alpha = 2.4$ for the FRII model and $\alpha = 2.2$ for the uniform model between a minimal energy $E_{\min} = 5 \cdot 10^{17}$ eV and a maximum energy $E_{\max} = Z \cdot 10^{22}$ eV. In this simulation, the cosmic ray component was normalized to the spectra from the Pierre Auger Observatory [16] at $5 \cdot 10^{18}$ eV which in turn determines the normalization of the secondary spectra.

While here we restrict ourselves to a simple example, a detailed study which aims at the prediction of the flux of secondary UHE-photons and neutrinos on the basis of CR-Propa 2.0 (beta) is presented at this ICRC [17].

3.2 3D: Composition and UHECR Astronomy

In 3D mode CRPropa can simulate deflections in EGMF. In LSS simulations with limited box size we apply cyclic boundary conditions on the surface of the simulation box such that a particle leaving through one side of the box is immediately injected at the opposite side of the next box. This approach generates automatically a background of far away sources if the maximum time that a UHECR will travel is chosen large enough.

In figure 2 we show a simulation with mixed composition of approximately $2 \cdot 10^6$ trajectories injected in a LSS magnetic field with a box size of $(75 \text{ Mpc})^3$, as in [20]. Inside the simulation box we placed 11 sources, 10 in an overden-

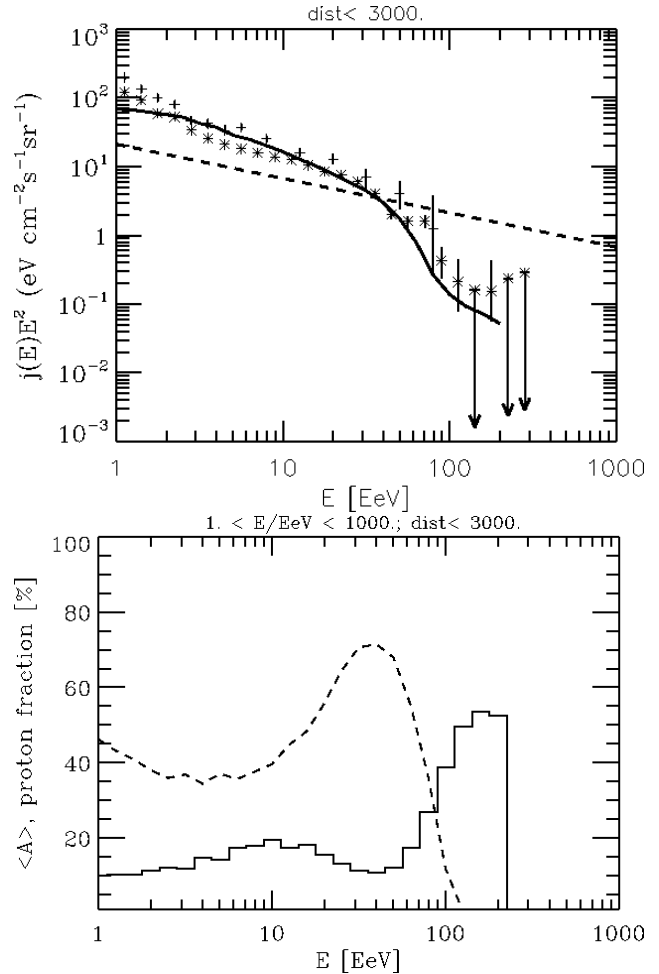


Figure 2: Simulated energy spectrum and mass composition in a 3D type simulation. In the upper panel the simulated cosmic ray spectrum (solid line) is compared with the spectra measured by HiRes [18] (crosses) and by the Pierre Auger Observatory [19] (stars). The straight dashed line represents the injected power law spectrum. In the lower panel the solid line shows the average mass while the dashed line shows the proton fraction as a function of energy. Details of the simulation are discussed in the text.

sity representing a galaxy cluster and one source considerably closer at a (CenA-like) distance of about 4 Mpc to generate anisotropy. This corresponds to a source density of $2.6 \times 10^{-5} \text{ Mpc}^{-3}$. With this setup, UHECRs with mixed composition were injected from the positions of the 11 sources and we applied weights to the individual trajectories later, such that the simulation represents a mixed composition with abundances following the galactic abundance [21]. In order to roughly fit experimental data, nuclei heavier than He were given a 10 times higher abundance than in the galactic composition. For the background sources we used a maximum energy $E_{\max} = Z \times 2 \cdot 10^{20}$ eV and a spectral index $\alpha = 2.5$, while for the nearby source we assumed a maximum energy $E_{\max} = Z \times 10^{19}$ eV and a spectral index $\alpha = 2.0$. The relative strength of the nearby source compared to the background sources is 10^{-2} . With

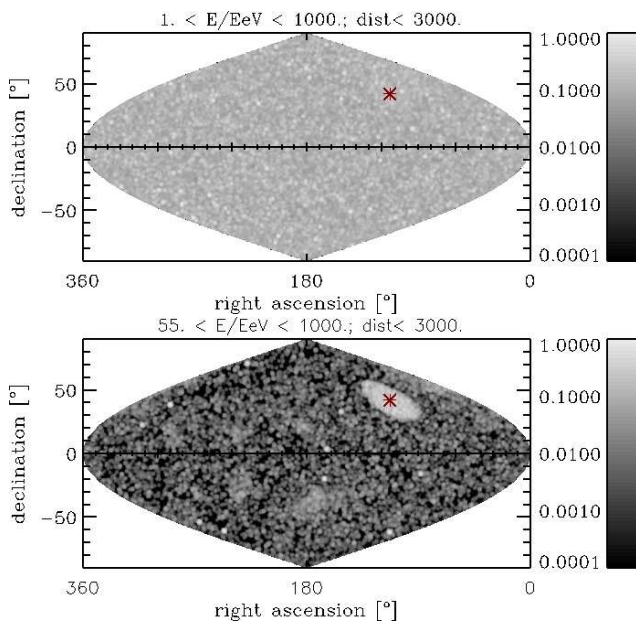


Figure 3: Skymap in sinusoidal equal-area projection of arrival directions above 1 EeV (top panel) and above 55 EeV (bottom panel) corresponding to the 3D simulation described in text. The position of the nearest source is marked by a star.

this setup, as it can be seen from figure 2, we achieve good agreement with the energy observed by the Pierre Auger Observatory and a heavier composition at higher energies [3]. Furthermore, as it is shown in the lower panel of figure 3, these parameter choices also allow an excess flux similar to the one observed at energies above ~ 55 EeV within about 20° from the direction of Cen A [3]. On the other hand, as clear from the upper panel of figure 3, at lower energies we obtain a sky that seems sufficiently isotropic to be in agreement with observations [3].

Both of these examples demonstrate how one can effectively apply CRPropa 2.0 in order to address open questions in UHE- ν , γ and cosmic ray physics: UHECR-astronomy, primary and secondary spectra (*multi-messenger approach*) and composition.

4 Summary and Conclusions

We briefly described the major changes applied to the publicly available version 1.4 of CRPropa to allow for the propagation of UHE-nuclei up to iron in the IGM. In exemplary simulations we outlined some useful features of CRPropa especially with respect to the primary spectrum, composition and anisotropies and we presented the spectra of neutrinos and photons in a Universe which undergoes cosmological evolution. Currently, a beta version of CRPropa 2.0 is being tested by external users. A more detailed description of the framework will be published when we release a public version of CRPropa 2.0.

5 Acknowledgments

We express our gratitude to all people who are helping beta testing. This work was supported by the DFG through the collaborative research center SFB 676. KHK and NN acknowledge financial support by BMBF under grant 05A08PX1. LM and GS acknowledge support from the State of Hamburg, through the Collaborative Research program “Connecting Particles with the Cosmos”.

References

- [1] J. Abraham *et al.* [Pierre Auger Observatory Collaboration], *Phys.Rev.Lett.* **104** (2010), 091101.
- [2] R.U. Abbasi *et al.* [HiRes Collaboration], *Phys.Rev.Lett.* **104** (2010), 161101.
- [3] P. Abreu *et al.* [Pierre Auger Observatory Collaboration], *Astropart.Phys.* **34** (2010), 314–326.
- [4] R.U. Abbasi *et al.* [HiRes Collaboration], e-print: arXiv:1002.1444 [astro-ph.HE] (2010).
- [5] E. Armengaud *et al.* *Astropart.Phys.* **28** (2007), 463–471.
- [6] S.R. Kelner and F.A. Aharonian, *Phys.Rev.* **D78** (2008), 034013.
- [7] G.R. Blumenthal, *Phys.Rev.* **D1** (1970), 1596–1602.
- [8] A. Mucke *et al.* *Comput.Phys.Commun.* **124** (2000), 290–314.
- [9] A.J. Koning, S. Hilaire, and M.C. Duijvestijn, *AIP* **769**, 2005, 1154.
- [10] J. Rachen, Phd thesis, “Universität zu Bonn”, 1996.
- [11] S. Agostinelli *et al.*, *Nucl.Instrum.Meth.* **A506** (2003), 250–303.
- [12] National Nuclear Data Center, <http://www.nndc.bnl.gov/nudat2/>.
- [13] J. V. Wall *et al.*, *A&A* **434** (2005), 133–148.
- [14] K. Kotera, D. Allard, and A.V. Olinto, *JCAP* **1010** (2010), 013.
- [15] A. A. Abdo *et al.* [Fermi-LAT Collaboration], *Physical Review Letters* **104** (2010) 101101.
- [16] J. Abraham *et al.* [Pierre Auger Observatory Collaboration], *Phys.Rev.* **D79** (2009), 102001.
- [17] Biswajit Sarka *et al.*, contribution #1341, 32nd ICRC (Beijing), 2011.
- [18] R. U. Abbasi *et al.*, *Astropart. Phys.* **32**, 53 (2009) [arXiv:0904.4500 [astro-ph.HE]].
- [19] J. Abraham *et al.* [The Pierre Auger Collaboration], *Phys. Lett. B* **685**, 239 (2010) [arXiv:1002.1975 [astro-ph.HE]].
- [20] Gunter Sigl, Francesco Miniati, and Torsten Ensslin, *Nucl.Phys.Proc.Suppl.* **136** (2004), 224–233.
- [21] M. A. Duvernois and M. R. Thayer, *Apj* **465** (1996), 982.